

Trapezoidal Volume Selection using Adiabatic Pulses

B. S. Park¹, and J. Shen¹

¹National Institute of Mental Health (NIMH), National Institute of Health (NIH), Bethesda, MD, United States

Introduction: Adiabatic pulses have been widely used in NMR spectroscopy and MRI applications because of their high RF magnetic field (B_1) insensitivity and excellent slice profile (1-4). Specifically, Sacolick *et al.* (1) recently showed selection of rectangular and octagonal volumes using adiabatic full passage (AFP) pulses. Instead of using a pair of identical adiabatic pulses necessary for obtaining full phase refocusing, Sacolick *et al.* found that significant phase refocusing can be achieved by executing single AFP pulses along non-equivalent spatial axes, therefore greatly reducing the number of AFP pulses needed for selecting non-rectangular volumes. Here we proposed an alternative scheme to directly select non-rectangular volumes by using a combination of stationary and time-varying slice-selection gradients.

Theory: It is well-known that an AFP pulse and a simultaneous stationary gradient can be used to select a slice with two parallel boundaries. When viewed in gradient vector space the slice boundary is perpendicular to the slice gradient vector while the integrity of the slice profile is governed by the adiabaticity of the AFP pulse. Therefore, if one changes the initial and final direction of the slice gradient vector and maintains adequate adiabaticity throughout the duration of the pulse a slice with non-parallel boundary can be generated. An example is shown in Fig. 1 where an orthogonal, linearly time-varying y antisymmetric gradient is added to a stationary x gradient during the execution of an AFP pulse. Such a scheme produces a symmetric nonparallel slice profile with the initial and final boundaries of the selected slice forming an angle $\theta = 2 \times \arctan(G_{y\max}/G_x)$. The “slice thickness” calculated at the gradient isocenter for zero carrier frequency offset is the same as the conventional slice thickness obtained without the time-varying gradient. Undoubtedly, the time-varying gradient puts a strain on the adiabaticity of the AFP pulse, which could be alleviated through numerical optimization of the adiabatic frequency sweep if necessary.

Results and Discussion: Figure 2 shows results of numerical simulation using Bloch equations without the relaxation terms and a two-dimensional sample space (20 x 20 cm). The well-known hyperbolic secant pulse was used without any modification. Pulse duration (T) = 3 ms, truncation level = 0.5%, $\gamma B_1 = 0.5 \times$ frequency sweep width, $\mu = 7.0$, $G_x = 2000$ Hz/cm, $G_y = 0$ or $G_{y\max} = 200, 400$ Hz/cm. Fig. 2 (a)-(b) shows calculated M_{xy} and M_z with $G_y = 0$. Fig. 2 (c)-(f) shows the calculated M_{xy} and M_z with $G_y = G_{y0}(1-2t/T)$. The simulated nonparallel slice profile (θ and “slice thickness”) matches theoretical predictions. A slightly increase in the width of the transition bands at the top and bottom of the trapezoidal slice profile can be seen as a result of degraded adiabaticity. This is expected since the transition band is known to be most susceptible to degradation in adiabatic behavior (At the point where the two slice boundaries meet, the pulse is expected to fail). In practice only the central portion of the slice profile shown in Fig. 2 (e)-(f) is needed, for example, when combining the scheme in Fig.1 with a second (pair of) AFP pulse(s) and a stationary G_y gradient to select a trapezoid. Fig. 3 shows additional variations in the G_y gradient waveform and corresponding changes in selected nonparallel slice profiles. Other choices of waveforms are also conceivable. In conclusion, we show that it is possible to directly select a nonparallel slice. Multiple such slices could be combined to form non-rectangular volumes for localized spectroscopy and spectroscopic imaging applications.

References

1. Sacolick *et al.*, MRM 2007; 57:548-553
2. Valette *et al.*, JMR 2007; 189 : 1-12
3. Kupce and Freeman, JMR 1996; 118, 299-303
4. Andronesi *et al.*, ISMRM 2009; p332

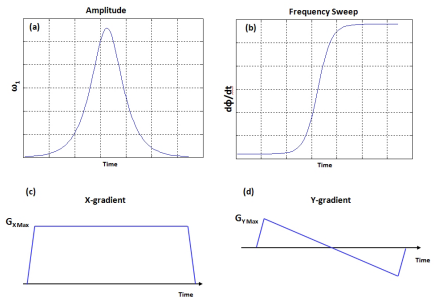


Figure 1 Designed RF pulse amplitude (a), frequency sweep (b), and gradient waveforms of x (c) and y (d).

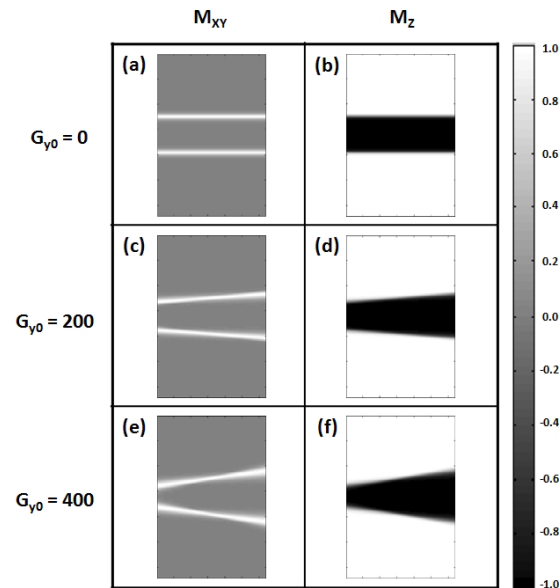


Figure 2 Numerical simulation results of the magnetization XY- (first column), and Z- (second column) with different Y-gradient strength (G_{y0}) of 0 (first row) 200 (second row) and 400 (third row).

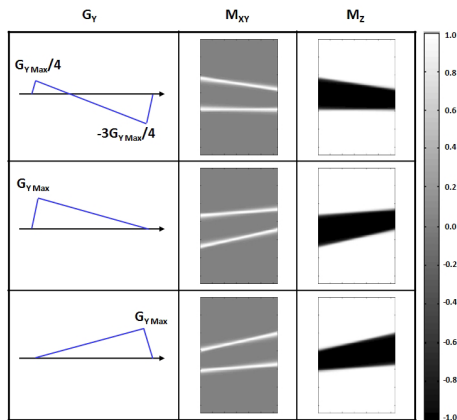


Figure 3 Numerical simulation results of the magnetization XY- (second column), and Z- (third column) with different Y-gradient waveforms.